

On-Surface Photochemistry of Pre-Ordered 1-Methyl-2-phenyl-acetylenes: C-H Bond Activation and Intermolecular Coupling on Highly Oriented Pyrolytic Graphite

Luciano Colazzo,*^[a, b] Maurizio Casarin,^[c, d] Mauro Sambi,^[c, e] and Francesco Sedona*^[c]

In this contribution we report on light-induced metal-free coupling of propynylbenzene molecular units on highly oriented pyrolytic graphite. The reaction occurs within the self-assembled monolayer and leads to the generation of covalently coupled 1,5-hexadiyne and para-terphenyl derivatives under

topological control. Such photochemical uncatalysed pathway represents an original approach in the field of topological C–C coupling at the solid/liquid interface and provides new insight into the low temperature formation of aromatic compounds at the surface of carbonaceous supports.

1. Introduction

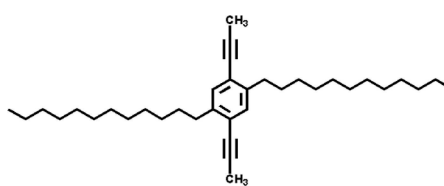
During the last years the photochemical on-surface synthesis approach has been successfully applied to some on-surface reactions (e.g. diacetylene polymerization,^[1] C–H^[2] and C–Br^[3] cleavage), with the purpose of producing covalently-bonded nanostructures at various interfaces.^[4] In some cases the chemical reactions are triggered on a pre-ordered self-assembled monolayer (SAM) of photo-sensitive molecules, since light irradiation preserves the favorable conformational arrangements of the molecular aggregates by limiting the diffusivity of the precursors that would normally occur by thermal activation. This scenario is generally referred to as topochemical control.^[5] Also an opposite approach has been recently reported by Para et al.,^[6] who obtained micrometer-long covalent organic fibers starting from monomeric precursors that form a disordered gas phase on the surface and that react through a UV photo-initiated radical within a chain-growth polymerization.

Light irradiation could in principle be used in hierarchical molecular coupling reaction strategies, since orthogonal activation mechanisms, e.g. heat and light, could be used, enabling the construction of complex functional nanostructures, while at the same time providing a better understanding of the reaction

pathways involved. However, despite these efforts, most of the on-surface reactions explored to-date are triggered mostly by thermal treatments^[7] or by STM tip manipulation,^[8] while the examples of light-induced on-surface reactions are still comparatively limited.^[9] As a matter of fact, the efficiency of the on-surface light-induced reactions tends to be very low, since in many cases the proximity of the substrate (metallic substrates in particular) provides relaxation pathways responsible for quenching the photo-excited species,^[10] with the immediate practical implication being that the chemical reactions are detectable only after many hours of irradiation. Nevertheless, the possibility to use non metallic surfaces like highly oriented pyrolytic graphite (HOPG)^[5a,9b] or calcite^[11] as substrates for photochemical synthesis was also successfully explored as a tentative solution for this bottleneck.

Although the alkyne group is a hot topic in the field of on-surface reactions, to-date exclusively terminal alkynes are known to give light-induced dehydrogenative coupling reactions both in UHV^[2] and in liquid environments.^[5a]

To the best of our knowledge the photochemical activation of methyl-acetylene groups within a SAM has never been explored experimentally. In this context, the present contribution confirms the potentialities of this functional group by reporting on the on-surface photo-reactivity of the propynyl (or methyl-acetylene) group ($-C\equiv C-CH_3$). A small π -system, namely 2,5-didodecyl-1,4-di-1-propynylbenzene, hereafter called ppBz (see Scheme 1), was used in order to attempt an on-surface photochemical coupling within its self-assembled monolayer on HOPG and in various environments.



Scheme 1. Structural formula of 2,5-didodecyl-1,4-di-1-propynylbenzene (ppBz)

[a] L. Colazzo
Center for Quantum Nanoscience, Institute for Basic Science (IBS), Seoul 03760, Republic of Korea
E-mail: colazzo.luciano@qns.science

[b] L. Colazzo
Department of Physics, Ewha Womans University, Seoul 03760, Republic of Korea

[c] M. Casarin, M. Sambi, F. Sedona
Dipartimento di Scienze Chimiche, Università di Padova, Via Marzolo 1, 35131 Padova (Italy)
E-mail: francesco.sedona@unipd.it

[d] M. Casarin
CNR-ICMATE, Via Marzolo 1, 35131 Padova (Italy)

[e] M. Sambi
Consorzio INSTM, Unità di Ricerca di Padova, Via Marzolo 1, 35131 Padova (Italy)

Supporting information for this article is available on the WWW under <https://doi.org/10.1002/cphc.201900382>

An invited contribution to a Special Issue on On-Surface Synthesis



The reaction occurred with high efficiency within a SAM and led to the generation of covalently coupled, mostly dimeric derivatives. The analysis of the reaction products suggests that the UV-promoted reaction pathways originate from the dissociation of propargylic C–H bonds,^[12] which initiate topochemically controlled recombination reactions leading to the formation of direct C–C bonds or to a phenyl ring between the self-assembled monomers.

Experimental Section

ppBz molecules purchased from Sigma Aldrich have been used without further purification. In order to perform the STM analysis at the solid/liquid interface, the molecules have been dissolved in heptanoic acid (hereafter 7COOH) or in phenyloctane (Ph8) at a concentration of 1 mg/g. A 5–15 µL droplet of solution was used for the observation of the interfacial behaviour of the solute at the solid/liquid interface. STM analysis at the solid/air interface were performed at room temperature (RT) by applying a 20–50 µL droplet of monomer solution in chloroform (CHCl_3) at a concentration of 1×10^{-4} M, allowing the solvent to evaporate prior to imaging (see SI section 1 for further details).

Surface preparation was performed by scotch tape cleaving of the HOPG surface and the surface cleaning was accurately checked prior to each deposition of the ppBz solutions. By drop-casting the solution at RT, relatively clean and stable samples were obtained, which remained unaltered for several days, although, to limit contamination induced by solvent evaporation, STM investigations were performed just after the completion of the drop-casting process.

The monochromatic light source used in this experiment was a tunable Nd:YAG laser system NT342 A-SH (EKSPLA) equipped with an optical parametric oscillator (OPO). Output energy at the 260 nm wavelength was 1.71 mJ, pulse frequency 30 Hz and pulse width 3.9 ns. (see SI, section 1, for further details).

2. Results and Discussion

Figure 1 shows representative images of the self-assembled phase of ppBz at the HOPG/7COOH interface: the molecules form extended lamellar structures characterized by distinct bright and dim contrast features. The same lamellar structure forms in Ph8 solution and at the solid/air interface (see SI,

Figure S1), although in the latter case some molecular vacancies are detected, and the overlayer islands undergo an irreversible degradation upon protracted raster scanning over the same region. This suggests that the overflowing solution at the liquid interface ensures the self-healing of the physisorbed monolayer by affording a dissolution–precipitation equilibrium.^[13]

The high-resolution image reported in Figure 1b shows that the monomers are planarly adsorbed within the lamella. The bright stripes can be attributed to the dipropynyl benzene cores with the two clearly visible propynyl arms,^[14] whereas the dark contrast region is associated to the dodecyl alkyl chains that interdigitate with the alkyl chains of the molecules belonging to the neighboring lamellae. Furthermore, high-resolution images in which both the substrate and the overlayer are present (see SI, Figure S2) allow us to determine that the bright stripes are parallel to the $\langle\bar{2}110\rangle$ substrate main directions, irrespective of the liquid/air environment. The distance between nearest neighbor molecules within a lamella is 0.95 ± 0.05 nm and – as already encountered for analogous molecules^[15] – the interdigitating chains spacing results in line with the required distance between two all-trans alkyl chains to match the HOPG in-plane lattice constant.^[16] The ppBz molecule can absorb with two enantiotopic faces and is therefore prochiral.^[17] Figure 1c reports an overlap of the molecular ball and stick model over a high resolution STM image in order to understand if the domain is homochiral or racemic. It is worth to point out that due to the intrinsic mobility of the molecules in the liquid phase, the position of the alkyl chains is not always well defined and therefore it is difficult to associate each molecule to one of the two enantiomers unambiguously. However, as reported in Figure 1c, it seems that molecules can indeed absorb with different enantiotopic faces and each domain is constituted by both the R and S enantiomers (represented with light and dark models, respectively). This is in contrast with previous studies on similar molecules, which report that an even number of carbon atoms within the alkyl chains generally promotes the formation of 2D enantiomerically pure conglomerates upon adsorption, whereas an uneven C number promotes racemic mixtures.^[18]

Several studies on the photolysis of simple organic molecules in the gas phase, such as propyne ($\text{H}-\text{C}\equiv\text{C}-\text{CH}_3$) and allene ($\text{H}_2\text{C}=\text{C}=\text{CH}_2$) isomers^[12a,b] demonstrated that UV photolysis can be used to produce propargylic radicals ($\text{H}-\text{C}\equiv\text{C}-\text{CH}_2\cdot$). These are known to play a key role in the formation of aromatic compounds and of polycyclic aromatic hydrocarbons both in high temperature flames during the combustion of aliphatic fuels^[19] and in evolved circumstellar environments in a wide range of temperatures,^[20] but also in low temperature planetary atmospheres.^[21] In particular, propargyl radicals may be generated in the gas phase in mild conditions by the photolysis of propyne, allene and of their halogenated precursors even at room temperature (295 K) and at pressures as low as a few Torr.^[22] The recombination chemistry of the propargyl radicals has been detailed experimentally and by density functional theory modelization, thereby finding a large number of products, the most interesting for our work being the barrierless formation of 1,5-hexadiyne ($\text{H}-\text{C}\equiv\text{C}-\text{CH}_2-\text{CH}_2-\text{C}\equiv\text{C}-\text{H}$) (HexD) –

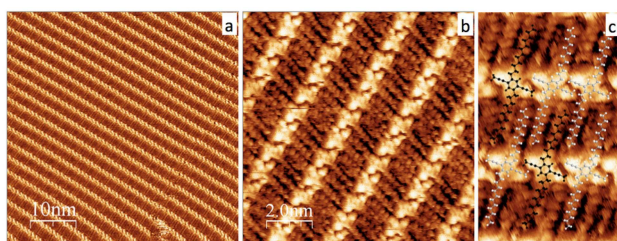


Figure 1. Topographic STM images of the self-assembled structures of ppBz molecules at the HOPG/7COOH interface: (a) large scale ($50 \times 50 \text{ nm}^2$, 1 V, 0.03 nA); (b) small scale ($5 \times 5 \text{ nm}^2$, -0.5 V , 0.021 nA); (c) zoom-in of Figure 1b with tentative overlap of molecular models of the two, differently colored, ppBz enantiomers.

the major product at room temperature^[21] – and the dimerization path leading to the closure of a benzene ring.^[19]

The formation of these two products are in fact confirmed also by the dimerization study of phenylpropargyl radicals ($C_6H_6-C\equiv C-CH_2$), a molecule more similar to our precursor. In this case the formation of the *para*-phenylene (p-Ph) ring leads to *para*-terphenyl ($C_6H_5-C_6H_4-C_6H_5$) as final product, whereas the formation of the dimers linked by HexD is suggested as the first step of the reaction mechanism that leads to the formation of 1-phenylethynyl-naphthalene.^[23]

In the case of ppBz molecules we provide evidence for the formation of dimers and oligomers connected by both HexD and p-Ph groups, as proposed in the reaction scheme reported in Figure 2. In order to achieve this, a UV-laser source tuned at

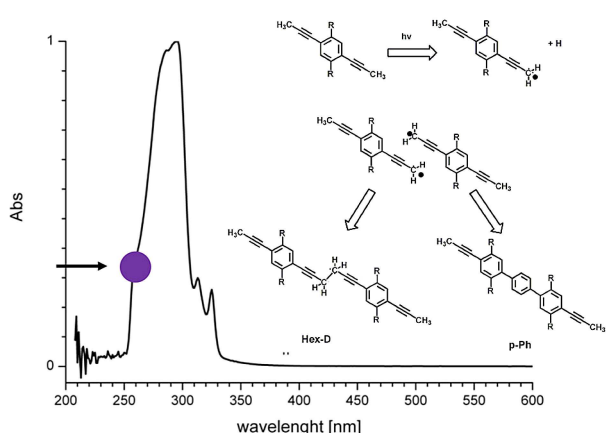


Figure 2. UV-Vis absorption spectrum in methanol solution of the ppBz molecule (the 260 nm wavelength is highlighted with a purple dot) and model of the dimers obtained from the propargyl radical formation.

260 nm has been chosen for the irradiation of the ordered lamellar system. The UV-Vis spectrum of ppBz in methanol solution shows an absorption band in the 250–350 nm region with a maximum at 296 nm (see Figure 2). This band is attributed to $\pi^* \leftarrow \pi$ transitions of the propynyl benzene core.^[24]

After 30 minutes of 260 nm laser irradiation, the ordered superstructure of ppBz in 7COOH transforms in a highly wavy aggregate (Figure 3a), where the previous uniform bright stripes become uneven and characterized by longer units and many interruptions. A careful inspection of the STM images indicates the formation of mostly dimers and some oligomers of the starting molecules (Figure 3b). The analysis of the dimers indicates that their structure is compatible with the formation of the HexD and p-Ph connections. Indeed, Figure 3c shows that the zoomed-in STM details of Figure 3b well match with the ball and stick models of the differently connected dimers and oligomers both in dimension and configuration.

In agreement with the observed racemic nature of the SAM reported in Figure 1c, dimers can in principle originate from the coupling of the same enantiomer, thus giving either the HexD_{RR(SS)} or the p-Ph RR(SS) configurations depending on the connection group, or from the coupling of different enantiom-

ers forming the corresponding HexD_{RS} or p-Ph_{RS} dimers. The monomers connected by the HexD group show an intermonomer distance of a 1.19 ± 0.05 nm, whereas the monomers linked by p-Ph rings are separated by 0.86 ± 0.05 nm.

Figure S3 of the supporting information reports a detail of Figure 3b with the corresponding ball and stick models. The assignment has been done comparing several consecutive images of the same area in order to discern the dimers from the oligomers. Although a certain degree of ambiguity in this assignment is unavoidable due to the limited STM resolution in the intrinsically dynamic liquid environment, it is clear that the majority of the STM features can be assigned, besides some remaining monomers, to the HexD_{RR(SS)} and to the p-Ph_{RS} dimers or oligomers, i.e. to three out of the possible six isomers listed above, while p-Ph homochiral and HexD heterochiral dimers are much rarer. The observed selectivity can be tentatively attributed to the reaction mechanism and/or to the compatibility of the dimers with the geometry of the self-assembled overlayer. Whereas the analysis of the reaction mechanism is beyond the scope of this work, we evidence that the geometry of the rarer dimers does not fit properly with the interdigitation geometry. Indeed, in the case of benzene homochiral dimers (p-Ph_{RR(SS)}) the distance between alkyl chains is around 0.8 nm, that is probably too short to allow the optimal inter-digititation, whereas in the HexD heterochiral dimers HexD_(RS) two alkyl chains are separated by about 1.3 nm, a distance too short to fit two alkyl chains in between and too large for an efficient accommodation of a single alkyl chain.

In this context, it is important to outline the evident similarity between the lamellar geometry of the starting SAM and the final covalent structure, which provides a strong indication that the photochemical reaction takes place at the preassembled molecular overlayer. It therefore appears that the reaction products are obtained under topochemical control by taking advantage of the proximity of the propynyl groups in the ppBz SAM (Figure 1c). This can easily explain the barrierless formation of the Hex-D links after the photochemical generation of the propargyl radicals.

On the other hand, the closure of the benzene ring previously reported to occur in the gas phase recombination of propargyl radicals, while representing the thermodynamic minimum for the system, is also associated to complex reaction pathways and with substantial computed activation barriers.^[19,25] However, the on-surface pre-assembly of the reactants is expected to substantially alter the reaction kinetics, both by reducing the absolute value of the steric contribution to the (negative) entropy of activation term, thereby increasing the reaction cross section, and – most importantly – by substantially altering the reaction potential energy surface. In fact, atomic hydrogen, which in our system is generated along with the propargyl radical by the initial photolysis step, is known to chemisorb on HOPG^[26] and could therefore be involved along with the substrate surface in the isomerization steps leading to the benzene ring closure along reaction paths substantially different from the gas phase reaction.

As reported in Section 3 of the SI, at the HOPG/air interface the reaction does not occur efficiently. Following the initial

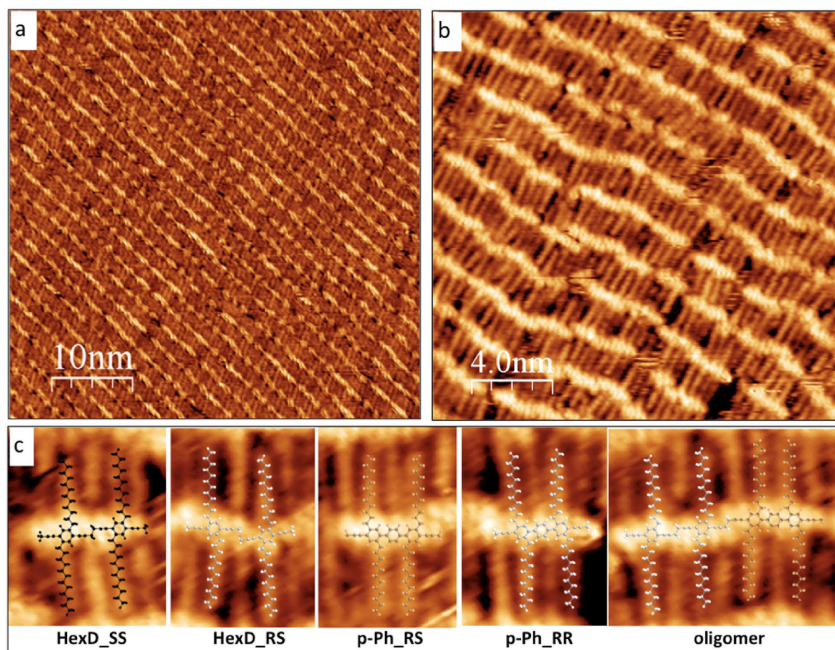


Figure 3. Topographic STM images of the ppBz molecules at the HOPG/7COOH interface after 30 minutes of 260 nm UV-laser irradiation: (a) large scale ($50 \times 50 \text{ nm}^2$, 0.6 V, 0.08 nA); (b) small scale ($20 \times 20 \text{ nm}^2$, 0.5 V, 0.03 nA), where dimers and oligomers are visible; (c) zoom-in of some details of (b) with tentative overlap of the dimers and oligomer models.

formation of ppBz dimers, mostly degradation and desorption occurs. In this case oxygen-mediated reactions are likely to occur,^[22a,27] on the photo-activated monolayer and unwanted oxidation necessarily hampers the desired intermolecular C–C coupling. On the other hand, at the HOPG/liquid interfaces, although low rate oxygen-mediated reactions are also known to occur,^[28] a larger amount of coupling-reaction products are obtained, characterized by the already highlighted wavy aggregation pattern on the large scale. Besides, the HOPG/7COOH interface was found to be the best environment for the photo-induced reaction. In this case, the solvent is transparent to the 260 nm radiation and the reaction is relatively fast, hence minimizing the ambient contamination of the sample.

To explore a possible thermal activation path for the coupling of the ppBz monomers, thermal annealing treatments were performed both at the HOPG/air and HOPG/liquid interfacial systems, but neither direct thermal activation nor synergic thermal and UV irradiation resulted in a successful intermolecular coupling. In the case of the HOPG/air interface, the thermal annealing was protracted up to 450 K, which represented the thermal degradation threshold of the monolayer, presumably because of the activation of air-induced oxidation reactions. Simultaneous thermal and UV irradiation induced desorption of the monolayer. For both the HOPG/liquid interfaces, providing thermal energy, with or without UV irradiation, resulted in the desorption of the ordered monolayer in favor of disordered and poorly resolved adsorbates.

3. Conclusions

This experiment demonstrates that on-surface photochemical coupling can be activated at the solid/liquid interface providing similar results to analogous systems studied under more stringent and metal-surface catalyzed UHV conditions.^[2] The photochemical activation affords high selectivity over the product distribution at short reaction times for a reaction that is unviable through thermal activation. Moreover, the photochemical activation gives a good control over the C–C bond formation when proper pre-assembly conditions are met and reactive species generated by photolysis are energetically driven to bond under topochemical control. Alkyl-chains in ortho-positions with respect to the photoactive propynylbenzene cores demonstrated to simultaneously offer a good stabilization of the 2D aggregates via cumulative supramolecular interaction networks, and also allowed the proper alignment of the molecular building blocks. As a drawback, this level of stabilization and the racemic nature of the preorganized SAM hindered a proper alignment of higher-order coupled precursors and the product distribution was limited to dimers or small oligomers. The coupling was triggered by direct molecular UV excitation and the reaction occurred in a catalyst- or cofactor-free environment, as occurs for alkyne homocoupling at the HOPG/liquid interface.^[5a] This substantiate the importance of a proper topological pre-organization in order to exploit the molecular reactivity via the photochemical approach as an alternative to the thermally activated reactions on metal surfaces. Finally, the proposed reaction paths involving the dimerization of photogenerated

propargyl radicals also shed new light into the low-temperature, carbon-supported generation of aromatic compounds, of potential interest in fields as diverse as environmental chemistry and astrochemistry.^[20]

Acknowledgements

The research leading to these results has received funding from the University of Padova (Grant CPDA154322, Project AMNES).

Conflict of Interest

The authors declare no conflict of interest.

Keywords: on-surface photochemistry • para-terphenyl • propargylic-like reaction • propynyl-benzene • scanning tunneling microscopy

- [1] a) Y. H. Qiao, Q. D. Zeng, Z. Y. Tan, S. D. Xu, D. Wang, C. Wang, L. J. Wan, C. L. Bai, *J. Vac. Sci. Technol. B* **2002**, *20*, 2466; b) X. Zhang, S. Xu, M. Li, Y. Shen, Z. Wei, S. Wang, Q. Zeng, C. Wang, *J. Phys. Chem. C* **2012**, *116*, 8950–8955.
- [2] H. Y. Gao, D. Zhong, H. Möning, H. Wagner, P. A. Held, A. Timmer, A. Studer, H. Fuchs, *J. Phys. Chem. C* **2014**, *118*, 6272–6277.
- [3] a) A. Basagni, L. Ferrighi, M. Cattelan, L. Nicolas, K. Handrup, L. Vaghi, A. Papagni, F. Sedona, C. Di Valentini, S. Agnoli *Chem. Commun.* **2015**, *51*, 12593–12596; b) Q. Shen, J. H. He, J. L. Zhang, K. Wu, G. Q. Xu, A. T. S. Wee, W. Chen, *J. Chem. Phys.* **2015**, *142*, 101902.
- [4] a) C. Guo, M. Li, S. Kang, *ChemPhysChem* **2016**, *17*, 802–811; b) H. L. Dai, Y. F. Geng, D. Q. Zeng, C. Wang, *Chinese Chem. Lett.* **2017**, *28*, 729–737; c) D. Frath, S. Yokoyama, T. Hirose, K. Matsuda, *J. Photochem. Photobiol. C* **2018**, *34*, 29–40.
- [5] a) L. Colazzo, F. Sedona, A. Moretto, M. Casarin, M. Sambi, *J. Am. Chem. Soc.* **2016**, *138*, 10151–10156; b) J. M. Njus, D. J. Sandman, L. Yang, B. M. Foxman, *Macromolecules* **2005**, *38*, 7645–7652.
- [6] F. Para, F. Bocquet, L. Nony, C. Loppacher, M. Féron, F. Chérioux, D. Z. Gao, F. Federici Canova, M. B. Watkins *Nat. Chem.* **2018**, *10*, 1112–1117.
- [7] a) Q. Sun, R. Zhang, J. Qiu, R. Liu, W. Xu, *Adv. Mater.* **2018**, *30*, 1705630; b) S. Clair, D. G. de Oteyza, *Chem. Rev.* **2019**, *119*, 4717–4776.
- [8] a) N. Pavliček, P. Gawel, D. R. Kohn, Z. Majzik, Y. Xiong, G. Meyer, H. L. Anderson, L. Gross, *Nat. Chem.* **2018**, *10*, 853–858; b) S. Clair, O. Ourdjini, M. Abel, L. Porte, *Chem. Commun.* **2011**, *47*, 8028; c) Y. Okawa, M. Akai-Kasaya, Y. Kuwahara, S. K. Mandal, M. Aono, *Nanoscale* **2012**, *4*, 3013;
- [9] a) A. Miura, S. De Feyter, M. M. S. Abdel-Mottaleb, A. Gesquière, P. C. M. Grim, G. Moessner, M. Sieffert, M. Klapper, K. Müllen, F. C. De Schryver, *Langmuir* **2003**, *19*, 6474–6482; b) D. Takajo, A. Inaba, K. Sudoh *Langmuir* **2014**, *30*, 2738–2744; c) X. Zhang, S. Xu, M. Li, Y. Shen, Z. Wei, S. Wang, Q. Zeng, C. Wang, *J. Phys. Chem. C* **2012**, *116*, 8950–8955; d) Y. H. Qiao, Q. D. Zeng, Z. Y. Tan, S. D. Xu, D. Wang, C. Wang, L. J. Wan, C. L. Bai *Nanom. Struct.* **2002**, *20*, 2466; e) A. Basagni, L. Colazzo, F. Sedona, M. Di Marino, T. Carofiglio, E. Lubian, D. Forrer, A. Vittadini, M. Casarin, A. Verdini, *Chem. Eur. J.* **2014**, *20*, 14296–14304.
- [10] a) X. Y. Zhu, J. M. White, *J. Chem. Phys.* **1991**, *94*, 1555; b) J. W. Gadzuk, *J. Chem. Phys.* **2012**, *137*, 091703; c) S. R. Hatch, X.-Y. Zhu, J. M. White, *J. Chem. Phys.* **1990**, *92*, 2681; d) S. Tognolini, S. Ponzoni, F. Sedona, M. Sambi, S. Pagliara, *J. Phys. Chem. Lett.* **2015**, *6*, 3632–3638.
- [11] A. Richter, V. Haapasila, C. Venturini, R. Bechstein, A. Gourdon, A. S. Foster, A. Kühnle, *Phys. Chem. Chem. Phys.* **2017**, *19*, 15172–15176.
- [12] a) C. K. Ni, J. D. Huang, Y. T. Chen, A. H. Kung, W. M. Jackson, *J. Chem. Phys.* **1999**, *110*, 3320; b) R. H. Qadiri, E. J. Feltham, N. Hendrik Nahler, R. Pérez García, M. N. R. Ashfold, *J. Chem. Phys.* **2003**, *119*, 12842; c) B. M. Broderick, N. Suas-David, N. Dias, A. G. Suits, *Phys. Chem. Chem. Phys.* **2018**, *20*, 5517–5529.
- [13] W. Song, N. Martsinovich, W. M. Heckl, M. Lackinger, *J. Am. Chem. Soc.* **2013**, *135*, 14854–14862.
- [14] K. S. Mali, K. Lava, K. Binnemans, S. De Feyter, *Chem. Eur. J.* **2010**, *16*, 14447–14458.
- [15] a) S. Taki, T. Kadotani, S. Kai, *J. Phys. Soc. Jpn.* **1999**, *68*, 1286–1291; b) K. Tahara, S. Furukawa, H. Uji-i, T. Uchino, T. Ichikawa, J. Zhang, W. Mamdouh, M. Sonoda, F. C. De Schryver, S. De Feyter, *J. Am. Chem. Soc.* **2006**, *128*, 16613–16625; c) S. Taki, H. Okabe, S. Kai, *Jpn. J. Appl. Phys.* **2003**, *42* (Part 1, No. 11), 7053–7056.
- [16] A. J. Groszek, *Proc. Roy. Soc. A* **1970**, *314*, 473–498.
- [17] J. A. A. W. Elemans, I. De Cat, H. Xu, S. De Feyter, *Chem. Soc. Rev.* **2009**, *38*, 722.
- [18] a) Y. Wei, K. Kannappan, G. W. Flynn, M. B. Zimmt, *J. Am. Chem. Soc.* **2004**, *126*, 5318–5322; b) H. Zhang, Z. Gong, K. Sun, R. Duan, P. Ji, L. Li, C. Li, K. Müllen, L. Chi, *J. Am. Chem. Soc.* **2016**, *138*, 11743–11748.
- [19] J. A. Miller, S. J. Klippenstein, *J. Phys. Chem. A* **2003**, *107*, 7783–7799.
- [20] C. Joblin, A. G. G. M. Tielen, I. Cherchneff, *Eur. Astronomical Soc. Publications Series* **2011**, *46*, 177–189.
- [21] A. Fahr, A. Nayak, *Int. J. Chem. Kinet.* **2000**, *32*, 118–124.
- [22] a) D. B. Atkinson, J. W. Hudgens, *J. Phys. Chem. A* **1999**, *103*, 4242–4252; b) J. D. DeSain, C. A. Taatjes, *J. Phys. Chem. A* **2003**, *107*, 4843–4850.
- [23] K. H. Fisher, J. Herterich, I. Fischer, S. Jaeq, A. M. Rijs, *J. Phys. Chem. A* **2012**, *116*, 8515–8522.
- [24] F. Ishii, S. Matsunami, M. Shibata, T. Kakuchi, *Polym. J.* **1999**, *31*, 84–88.
- [25] H. J. Singh, N. K. Gour, *Indian J. Chem.* **2010**, *49B*, 1565–1570.
- [26] a) L. Hornekaer, Ž. Šljivančanin, W. Xu, R. Otero, E. Rauls, I. Stensgaard, E. Lægsgaard, B. Hammer, F. Besenbacher, *Phys. Rev. Lett.* **2006**, *96*, 156104; b) H. González-Herrero, E. Cortés-del Río, P. Mallet, J.-Y. Veuillet, J. J. Palacios, J. M. Gómez-Rodríguez, I. Brihuega, F. Ynduráin, *2D Mater.* **2019**, *6*, 021004.
- [27] Y. Sohn, W. Wei, J. M. White, *J. Phys. Chem. C* **2008**, *112*, 18531–18536.
- [28] D. den Boer, M. Li, T. Habets, P. lavicoli, A. E. Rowan, R. J. M. Nolte, S. Speller, D. B. Amabilino, S. De Feyter, J. A. A. W. Elemans, *Nat. Chem.* **2013**, *5*, 621–627.

Manuscript received: April 15, 2019

Revised manuscript received: June 3, 2019

Accepted manuscript online: June 27, 2019

Version of record online: August 6, 2019